

# Mine detection with ground penetrating synthetic aperture radar

Marshall Bradley<sup>a</sup>, Thomas Witten<sup>b</sup> Robert McCummins<sup>a</sup>, Michael Duncan<sup>a</sup>

<sup>a</sup>Planning Systems Incorporated, Long Beach, Mississippi

<sup>b</sup>U.S. Army Night Vision and Electronic Sensors Directorate, Ft. Belvoir Virginia

## ABSTRACT

In order to detect buried land mines in clutter, Planning Systems Incorporated has developed a Ground Penetrating Synthetic Aperture Radar (GPSAR) system for the U.S. Army CECOM Night Vision and Electronic Sensors Directorate. The GPSAR system is a wide-band stepped-frequency radar operating over frequencies from 500 MHz to 4 GHz. Our GPSAR uses multiple transmit and receive antennas to acquire data at 58 across-track locations separated by 1.47 inches. Along-track data sampling is provided by the forward motion of the system. Multiple radar channels and high-speed radio frequency switching are used to accelerate the data acquisition process and increase the system's maximum speed of advance. Synthetic aperture, near-field beamforming techniques are used to reduce clutter and enhance the signature of buried objects. While the system is designed for mine detection it is capable of locating deeper objects such as buried utility pipes. Tests conducted in December 2001 at U.S. Army facilities indicate that the system can detect both metallic and plastic landmines at depths up to 6 inches. A description of the PSI GPSAR system and test results are presented.

**Keywords:** Ground Penetrating Radar, Synthetic Aperture, Mine Detection

## 1. INTRODUCTION

The detection and neutralization of buried landmines has become an increasingly important issue as military forces rely more than ever on increased mobility. Land mine threats slow the advance of fighting units and complicate logistical operations behind friendly lines if left un-neutralized. The landmine threat is especially acute in regions such as Bosnia and Afghanistan where mountainous and rugged terrain restricts maneuverability. To facilitate route clearance in these areas some method of individual mine detection and neutralization is required.

At present mine-detection and mine-clearance technology consists primarily of metal detectors, probes, and tank-mounted flails or similar vehicles. The need to detect plastic-cased, minimum-metal content mines without significantly impairing mobility and damaging road surfaces, however, is not fully met by these types of systems. Ground penetrating radars (GPRs) have been used as a non-intrusive means of landmine detection for several years. They have a demonstrated ability to detect both plastic and metal landmines but generally suffer from a high probability-of-false-alarm (Pfa) due to their susceptibility to clutter. Additionally most GPR systems operate in a "ground-coupled" configuration with their antennas very close to or resting on the ground surface in order improve penetration. While this increases the SNR of the radar it is a difficult configuration to adapt to a fast moving vehicle over rough terrain.

Our GPSAR system differs from others in several ways. Firstly it uses small diameter yet broad-band archimedean spiral antennas. This allows for a denser array packing that improves spatial resolution. Second we use fully coherent synthetic aperture processing techniques to increase SNR and reduce the adverse effects of clutter. Third our GPSAR is able to operate in a non ground-coupled mode and still detect buried targets.

The remainder of this paper describes our GPSAR system and presents the results of tests conducted at U.S. Army field sites.

---

Further author information E-mail: bradley@psislidell.com, Telephone: 1.985.649.0450



**Figure 1.** GPSAR at U.S. Army test site. System components visible in this photograph include the front and rear antenna arrays (A), RF switches (B), and radar module electronics (C).

## 2. SYSTEM OVERVIEW

Photographs of the GPSAR system as configured in December 2001 are shown in Fig. 1 and Fig. 2 and a system block diagram is shown in Fig. 3. The vehicle is a modified electric turf vehicle capable of maintaining a steady speed of advance under local or remote control. Primary system components include two antenna arrays, two sets of radar electronics called *radar modules*, two 16-position high speed radio frequency switches, an AC auxiliary power box, a DC power distribution box, a rack-mount industrial PC, a laptop PC, wireless Ethernet hardware and a GPS receiver. Each set of radar electronics is used to drive a single antenna array. The industrial PC, mounted in the bed of the vehicle in a water-resistant case, is used to coordinate data acquisition and processing. The laptop PC provides an interface to the industrial unit when the case is sealed.

The across-track resolution is a fixed function of the array antenna spacing, while sampling in the along-track direction is provided by the forward motion of the system and may be varied. As the system moves forward, an optical encoder is used to determine the distance traveled. When a multiple of the prescribed along-track sampling interval is reached the industrial PC initiates a data acquisition cycle on each of the two radar modules. A single acquisition cycle collects the full set of frequency data from all transmit/receive antenna pairs in an array. This data is then logged on the industrial PC and sent into the processing stream.

## 3. SYSTEM COMPONENTS

### 3.1. Antennas

A view of the Archimedean spiral antennas is shown in Fig. 4 along with our previous log-spiral design. The Archimedean antennas, shown on the right, were designed based on consultation with engineers at the Naval Weapons Center, China Lake. They have much higher gain (10 - 15 dB) than the log-spirals and better far-field beam patterns. While these antennas were designed to operate over 800 - 4000 MHz they radiate well down to 500 MHz. Each antenna is cavity backed in a thin-walled 9"L x 5.75"D aluminum cylinder. The cylinders are filled with radar absorbing material to attenuate upward radiated energy. A layer of Styrofoam separates the absorbing material from the antenna circuit board material and a Delron face-plate is mounted over the opposite radiating surface to prevent abrasion or other damage.

The traces imprinted on the antenna face of the Archimedean spirals expand in a linear fashion. This allows for longer antenna arms than with the log-spiral but does induce some frequency dependent phase effects. These



**Figure 2.** GPSAR at U.S. Army test site. System components visible in this photograph include antenna arrays (A), radar module electronics (B), auxiliary AC power box (C), rack-mount equipment case (D), and the laptop computer (E).

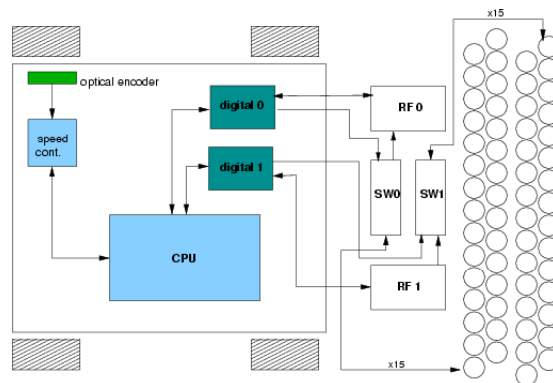


**Figure 3.** Block diagram of major GPSAR components. The primary CPU handles signals from the speed controller board which monitors the optical encoder. The digital boards feed the 10.7 MHz reference signal to the RF boards and control the switches.

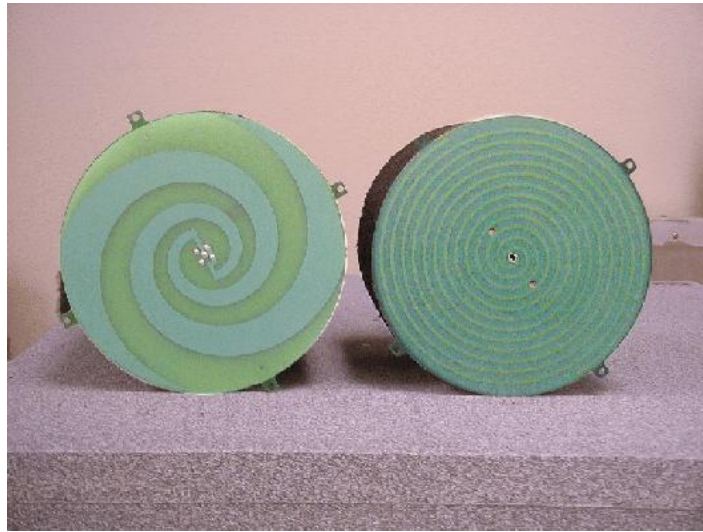


**Figure 4.** GPSAR Antennas. Previous versions of the GPSAR used log-spirals (left) abandoned in favor of archimedean spirals (right). The antenna arms are etched into printed circuit board material. Not shown are a microstrip balun used to balance current on the arms and resistive terminators at the end of each arm.

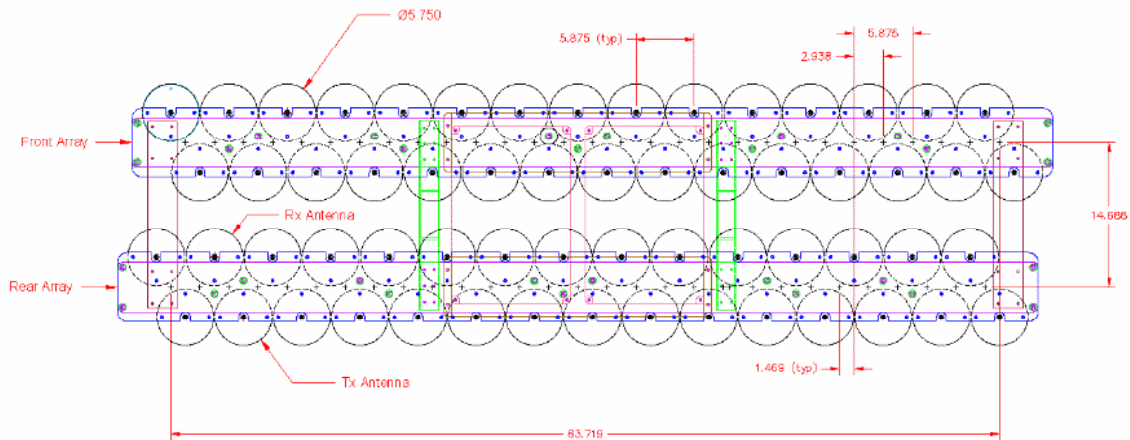


**Figure 5.** Top down view of the front (upper) and back (lower) antenna arrays. Each bank contains fifteen transmit and fifteen receive antennas. The front antenna bank is offset 1.47 inches to the right of back antenna bank in order to improve overall system spatial resolution.

are removed during processing. A microstrip balun is used to balance the current on each of the antenna arms and to improve the impedance matching between the antenna and the connecting coaxial cable.

A top down schematic of the back and front antenna arrays is shown in Fig. 5. The antenna centers are 5.875 inches apart when mounted on the frame. On each array antennas in the bottom (rear) row serve as transmitters while those in the top (forward) row act as receivers. Transmit and receive antennas have opposite windings to minimize direct coupling.

The nested configuration shown in Fig. 5 was chosen to maximize spatial resolution in the across-track, or





**Figure 6.** Front view of the GPSAR system. The RF switches (A) are mounted in the center immediately above the antennas. The RF portions of the radar modules (B) are mounted next to the switches on either side of the frame.

$x$ , dimension. Resolution in the along-track, or  $y$ , dimension is configurable. A source "sharing" scheme is used during data acquisition whereby a single transmitter is used to drive each of its adjacent receivers in sequence. This provides 29 source/receiver combinations or "channels" per array. The  $(x, y)$  coordinates of the focal points used in beamforming lie at the mid-points of lines connecting the source and receive antenna centers. A 30th channel connects the radar transmit line directly to the radar receive line through an RF attenuator. Data from this channel is used to monitor performance and remove system dependent artifacts.

The antenna centers in each array are spaced 5.875 inches apart which separates the focal points by 2.938 inches in the across-track direction. The front and back arrays are offset in relation to each other by half the focal point separation to make the overall across-track resolution of the system approximately 1.47 inches. During operation the user may elect to view the output of a single radar-module/array combination or the combined output of both arrays and modules.

The antenna arrays are mounted on a height adjustable frame as shown in Fig. 6. The RF cables in the figure connect the individual transmitters and receivers to the switches. Each cable is cut to the same length to prevent differences in switch-to-antenna travel time.

### 3.2. Radar modules

At the heart of the GPSAR system are two sets of single-channel, digitally controlled stepped-frequency radar modules. An all digital modulator coupled with a coherent digital quadrature FPGA based receiver is used for making precise magnitude and phase measurements. Each radar module consists of two major components shown in Fig. 7 and Fig. 8. The first, called the digital or IF board, handles all communication, controls the RF switches and measures magnitude and phase. The second, called the radar or RF, section generates and receives the actual RF signals that are fed to the antennas. The digital and RF sections are contained in separate housings, the radar sections in custom built low noise enclosures near the antenna arrays, and the digital boards in rack-mount boxes in the computer case.

Key digital board components include an embedded micro-processor, an Ethernet chipset, a Direct Digital Synthesizer (DDS), a Digital Down Converter (DDC) and a Digital Signal Processor (DSP). The radar section is comprised of a set of band-pass and low-pass filters, local oscillators, mixers and a YIG variable frequency oscillator.

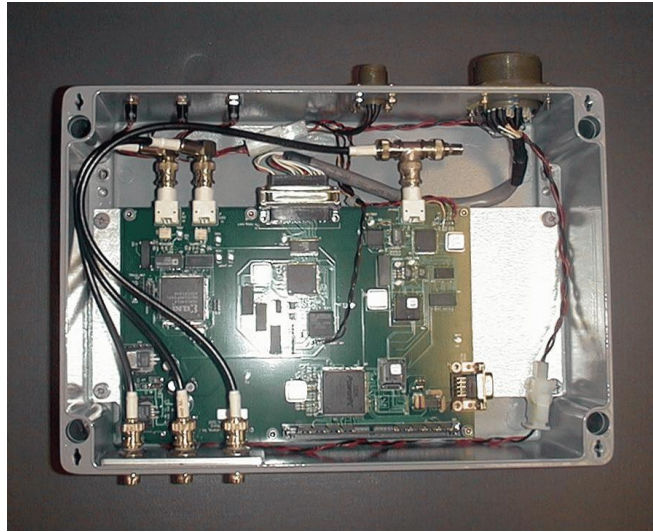


**Figure 7.** GPSAR Digital board. The digital board has four primary functions 1) control the RF switches, 2) supply 10.7 MHz analog signal to the RF boards, 3) control the RF YIG oscillator and 4) make precise phase measurements. the RF boards

For given given frequency and channel pair transmission and reception occur simultaneously. When an acquisition is initiated, an analog 10.7 MHz reference signal is generated on the digital board and sent to the radar section via coaxial cable. The radar section then steps the 10.7 MHz signal up in frequency through a series of mixers and local oscillators. The last mixing stage beats against the output of a YIG variable frequency oscillator controlled by the digital board. By varying the frequency of the YIG oscillator the RF output may be stepped between 500 MHz and 4.0 GHz. The RF switches, also controlled by the digital board, are then used to connect the radar output and input to the appropriate transmit/receive antenna pair. The received signal is passed through the same set of mixers and oscillators this time stepping the signal back down in frequency to 10.7 MHz. To increase efficiency all transmit/receive combinations are polled before switching the YIG frequency. The digital board then performs I/Q demodulation on the received signal using the original 10.7 MHz reference. I/Q pairs are averaged in the DSP and made available via the TCP/IP connection when all frequencies have been acquired.

### 3.3. Mechanical assembly

The radar platform shown in Fig. 1 and Fig. 2 is a modified John Deere turf vehicle. The vehicle carries all system hardware and is electrically powered by eight 12V batteries, requiring no umbilical. The vehicle may be operated in local or remote modes. Battery life may be up to 8 hrs. depending on the load drawn by increased operating speed and/or terrain. An additional AC power box was constructed to supply AC voltage to on board computers and other equipment. The radar antennas are mounted on the front of vehicle on a specially constructed motor-controlled frame that may be used to lower or raise the antennas over a 12" vertical range. The RF boards and high speed switches are housed on enclosures mounted on the antenna frame minimizing the required RF cable lengths. The digital boards and the primary on board computer are housed in a watertight rack-mount case located in the bed of the vehicle, between the seats and the AC power box. A second on-board laptop computer connected via Ethernet to the main computer is mounted in the cab. This allows the watertight case to be sealed during operation. An additional speed controller board was designed and interfaced with the electric drive motors to help maintain a constant speed of advance. An optical encoder is mounted to a dedicated shaft that couples to the left, rear drive wheel through a sprocket and chain assembly. This encoder is used to determine forward distance traveled based on wheel diameter and the number of encoder counts per revolution. Revolutions of the encoder are monitored by the speed controller board. When a prescribed distance has been

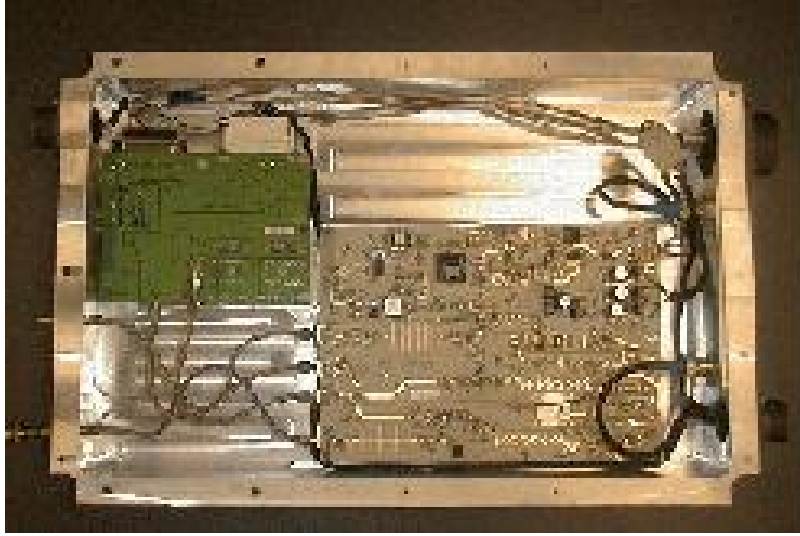


**Figure 8.** GPSAR RF, or *radar* section. Each RF section consists of two printed circuit board components 1) YIG board (upper left) and 2) mixing board (lower right). The mixing board is populated with the various mixers oscillators and filters required to bring the 10.7 MHz digital board signal into the 0.5 - 4.0 GHz range. The YIG board supports the variable frequency YIG oscillator that feeds the final mixing stage.

traveled the speed controller board sends a hardware interrupt to the main computer via the parallel port which then initiates data acquisition by the radar modules.

A canopy was constructed to protect the electronics in the bed and to provide shade over the seats. The front suspension was modified to facilitate the heavy antenna array and a 4:1 gear reducer was installed to allow slow speeds of advance. The new gear box installation required the re-location of the main drive motor.

The vehicle can operate in either local or remote control mode. A motor-controlled chain drive was attached to the existing steering column for remote steering.

## 4. GPSAR DATA SAMPLING AND PROCESSING

### 4.1. Data sampling

Frequency data are sampled over a two dimensional grid. Acquisition cycles are initiated at user defined spatial intervals in the along-track direction. On every acquisition cycle or scan, each radar modules steps through all  $N_f$  frequencies and across all  $N_c$  transmit/receive antenna combinations. As the system advances a two-dimensional grid suitable for SAR processing is produced. Discarding the first ten scans received by the back array, data from both arrays may be interleaved to effectively double the across-track resolution. This is made possible by the across-track offset of the two arrays.

Taking  $x$  to be the across-track direction and  $y$  to be the along-track direction and  $z$  to be vertical depth or time direction, the  $(x, y)$  coordinates used in the SAR focusing procedure lie at the mid-points of lines connecting transmit and receive antenna centers. These are called focal points, or *channels*. Each array provides 29 data channels based on the sharing of any transmitter between adjacent receivers.

The recorded data is an array of complex numbers of the form  $\psi(m, n, p)$  where  $m$  is the cross- track index ( $0 < m < N_c - 1$ ),  $n$  is the along-track or scan index and  $p$  is the frequency index ( $0 < p < N_f - 1$ ). The quantity  $\psi(m, n, p)$  represents the complex frequency response of the ground at the location  $(x, y) = (mdx, ndy)$  where  $dx$  and  $dy$  are the across-track and along-track sampling intervals respectively. The Fourier transform of  $\psi(m, n, p)$  over  $p$  is the equivalent time domain response of the radar at  $(x, y)$ .

## 4.2. Pre-processing

The GPSAR data contains several system related artifacts that can be removed in pre-processing stages without affecting the relevant mine-echo information.

One artifact is a constant positive offset in the real and imaginary components of the frequency data removed by simply subtracting the offset across all frequencies. A second is the delay induced by the system cables. In order to properly locate mines in time/depth the data must be shifted forward in time to account for propagation through the cabling. Multiplying by  $e^{2\pi i f_p \tau_{cable}}$  accounts for this where  $\tau_{cable}$  is the known cable travel time. A similar effect occurs in the RF switches however the required time shift is a function of channel. This results from the switch ports having different electrical path lengths.

The antennas themselves are frequency dispersive, higher frequencies radiating from near the center and lower frequencies from farther out on the antenna arms. A frequency dependent time delay is required to account for the resulting differences in propagation time. This delay is well described mathematically based on the known antenna geometry. In practice the delays due to cable length, switches, and antennas may be removed in one complex multiplication of the form:

$$\hat{\psi}(m, n, p) = \psi(m, n, p) e^{i2\pi f_p (\tau_{cable} + \tau_{switch}(m) + \tau_{antenna}(p))} \quad (1)$$

where  $\hat{\psi}(m, n, p)$  is the corrected frequency domain data.

The radar electronics do not produce a spectrum that is entirely flat. Amplitude modulation in the frequency domain will produce side-lobes in the time domain that complicate interpretation and may obscure targets. To account for this the frequency output of the radar modules is recorded along with the data for each scan. This *calibration* channel is used to scale the data received through the antennas and remove the radar module amplitude and frequency modulation.

## 4.3. SAR

To determine the magnitude of the radar response at a given focal point at  $(x, y)$  and depth  $z$  data obtained by multiple adjacent transmit/receive pairs are used in a delay-sum SAR focusing algorithm given by:

$$I(x, y, z) = \Delta f \sum_{p=0}^{p < N_f} \sum_{\mu=-M_s}^{\mu=+M_s} \sum_{\eta=-N_s}^{\eta=+N_s} \psi_{m+\mu, n+\eta, p} e^{2\pi i f_p \tau_{m+\mu, n+\eta}(mdx, ndy, z)} \quad (2)$$

The integers  $\mu$  and  $\eta$  are the indices of adjacent data channels. The limits  $M_s$  and  $N_s$  determine the  $x$  and  $y$  extent of the spatial array. The delay  $\tau$  is the time required to propagate from the transmit/receive pair at  $((m+\mu)dx, (n+\eta)dy)$ , to the focal point  $(x, y, z)$  and back accounting for refraction at the ground surface. The resulting 3D data set is referred to as the radar *image*. Typically maximum values are taken along the  $z$  and  $x$  dimensions to produce 2D images in the  $x - y$  and  $y - z$  planes respectively.

## 4.4. Spatial filtering

In order to reduce the masking effects of the ground bounce return and other constant noise sources the radar data is spatially high-pass filtered in the along-track direction. Spatial filtering may be applied prior to beamforming or after the data has been converted to the time/depth domain. Early experiments showed that in some cases subtracting an average value taken over several scans for each channel and frequency sample improved the image SNR considerably. Assuming any buried targets occupy a small region of the selected averaging space, this so-called *average differencing* in effect removes the mean background noise. If the background noise remains fairly constant over the averaging space the radar image SNR is enhanced. However if the noise does not remain constant the subtraction can introduce false returns in regions that deviate significantly from the mean. Spatially non-uniform clutter easily produces such artifacts as does the return from the air/ground interface when the surface is not flat.



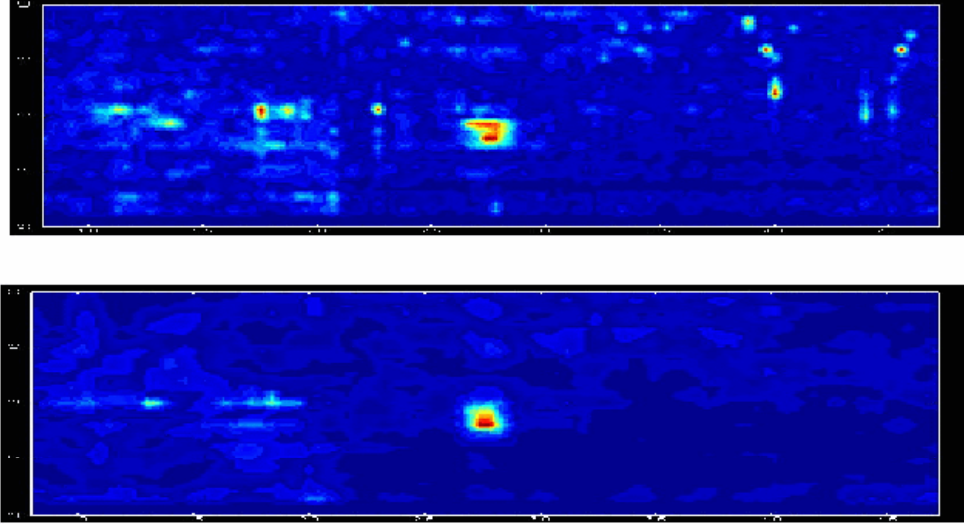


**Figure 9.** Effects of SAR processing. A top down image of a buried TM62M mine is shown before (above) and after (below) SAR beamforming with a 3x5 array. The SNR is improves as clutter is reduced.

To help mitigate the artifacts caused by simple average differencing and retain the improved SNR we have employed a modified subtractive technique called *adaptive differencing*. The key to this procedure is the assumption that nearby scans will have similar ground bounce returns, and thus can be used to approximate the ground bounce of the current scan as follows.

Fix the channel,  $m$ , and let the frequency data for scan  $n$  be

$$G_{m,n,p} \in C \quad \forall p = M_1, \dots, M_2. \quad (3)$$

Let  $N_{filter}$  be the filter window size and  $N_{mine}$  be the size of the buffer region for potential mines. Let

$$B_{filter} = \left\{ n - \left\lfloor \frac{N_{filter}}{2} \right\rfloor, \dots, n + \left\lfloor \frac{N_{filter}}{2} \right\rfloor \right\} \cap \{N_1, \dots, N_2\}$$

be the scans within  $N_{filter}$  of the current scan,  $n$ . Similarly, let

$$B_{mine} = \left\{ n - \left\lfloor \frac{N_{mine}}{2} \right\rfloor, \dots, n + \left\lfloor \frac{N_{mine}}{2} \right\rfloor \right\} \cap \{N_1, \dots, N_2\}$$

be the scans within  $N_{mine}$  of the current scan,  $n$ . Adaptive differencing uses the scans in  $B_{filter} \setminus B_{mine}$  as potential ground bounce references for scan  $n$ .

For each scan  $\nu \in B_{filter} \setminus B_{mine}$ , define the correlation between scans  $n$  and  $\nu$  by

$$\rho_n(\nu) = \frac{\left| \sum_{p=M_1}^{M_2} G_{m,n,p} G_{m,\nu,p}^* \right|}{\left( \sum_{p=M_1}^{M_2} |G_{m,n,p}|^2 \sum_{p=M_1}^{M_2} |G_{m,\nu,p}|^2 \right)^{1/2}} \quad (4)$$

Let  $\mu \in B_{filter} \setminus B_{mine}$  maximize  $\rho_n(\mu)$ . Scan  $\mu$  is the most highly correlated reference for the ground bounce in scan  $n$ ; consequently, it is subtracted from scan  $n$  to remove the ground bounce return:

$$G_{m,n,p}^{new} = G_{m,n,p} - G_{m,\mu,p} \quad \forall p \in \{M_1, \dots, M_2\}. \quad (5)$$

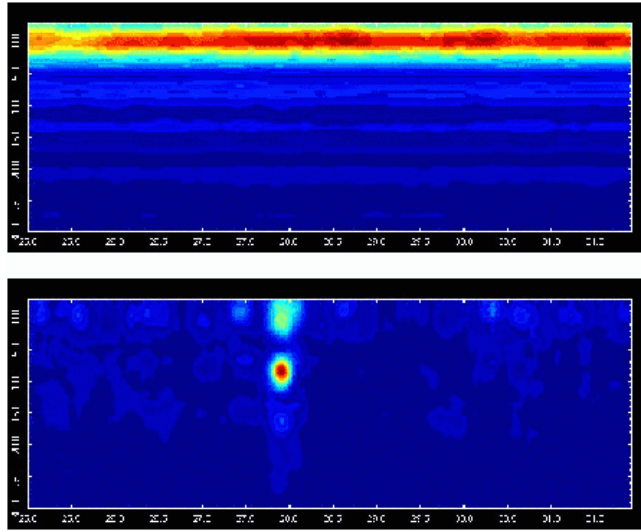


**Figure 10.** Effects of adaptive differencing. A side view, or  $x-z$  plane, image of a buried TM62P is shown before (above) and after (below) the removal of masking background noise using the adaptive differencing process.

Landmines often appear in the data as regions of *decreased* radar echo level, or "dark spots" in the image. When this occurs the mine signature may be occluded by higher background noise levels. This is the case shown at the top of Fig.10 where a buried plastic TM62P anti-tank mine is completely hidden by masking background noise. The application of the adaptive differencing filter produces the image shown in the bottom of Fig.10. The removal of constant background noise reveals the echo-level anomaly caused by the presence of the mine as an easily interpreted "bright spot" in the image.

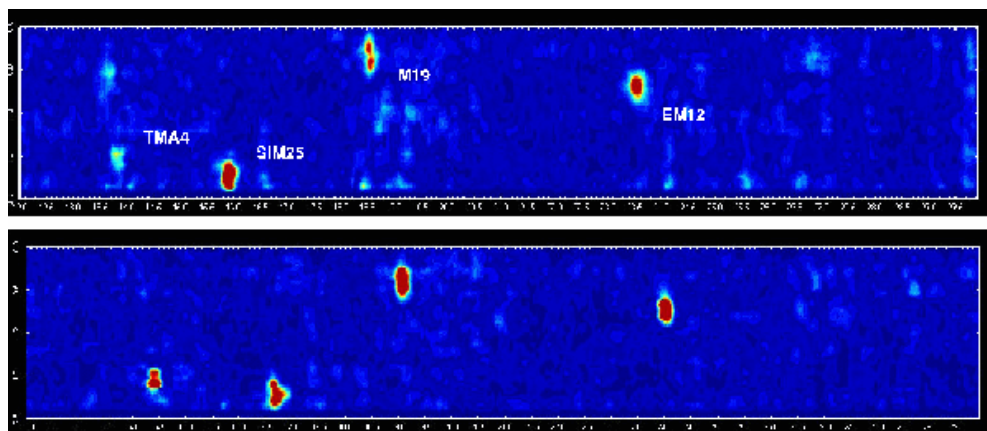
## 5. GPSAR PERFORMANCE

Fig.11 and Fig.12 show the performance of the GPSAR system at a U.S. Army test facility in December 2001. Top down, or  $x-y$  plane, view are shown of a section of one of the test mine lanes in each of the figures. All pre-processing steps, adaptive differencing and SAR processing were applied to produce the images shown. Weather at the test site was wet after two months with no appreciable precipitation. While it is generally believed that increased soil moisture improves GPSAR performance. Our results, however, indicate that moisture collected at the surface inhibits penetration of the radar energy by increasing the soil/air dielectric contrast. The overall system performance is thus somewhat degraded when the antennas are elevated over wet ground.

Fig.11 shows the effectiveness of the GPSAR system against buried anti-tank mines. All of the mines shown in the figure are plastic cased and there are no other mines in this test lane section which the GPSAR did not detect. In the upper image the antennas were raised twelve inches above the ground surface. All the mines are detected with a possible false alarm near the upper left corner of the image. In the lower image the antennas were lowered to two inches above the surface. As expected the SNR is improved and the potential false alarm disappears, however the detection results are the same.

In Fig.12 the effects of mine composition and burial depth are shown. The metal cased TM62M on the left has a much sharper dielectric contrast with the surrounding soil and makes a stronger target than the plastic TM62Ps. While the difference in received signal strength between metal and plastic mines is generally quite large the GPSAR dynamic range and clutter reduction methods allow the detection of both.

The TM62P on the right, although buried deeper, in Fig.12 has a larger signature than the center TM62P whose top is flush with the ground surface. This is attributed to interference effects or masking by the echo from the ground surface. While the GPSAR is generally better at detecting deeper targets, the increased bandwidth of the system has significantly improved performance against shallow mines.



**Figure 11.** Top down view of mines detected at U.S. Army test site. All the mines in this section of the test lane are plastic cased. Burial depths are: TMA4, 2"; SIM25, 2"; M19, 5"; and EM12, 1". Upper image is with antennas 12" above the surface, lower image is with antennas 2" above the surface.

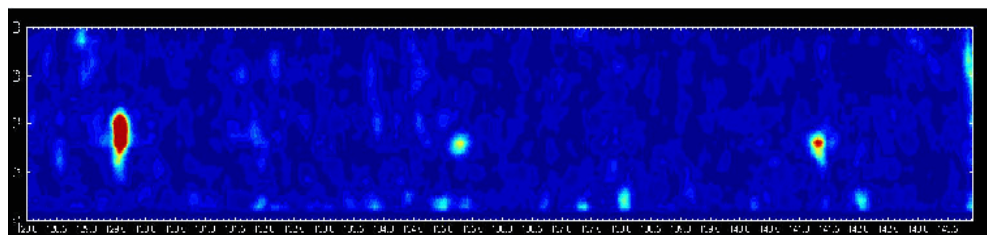


**Figure 12.** Top down view of mines detected at U.S. Army test site. The metal cased TM62M buried at 15 cm has a much larger signature than the plastic cased TM62P mines on the right. The center TM62P has a smaller signature than the TM62P on the right which is buried at 15 cm. This is likely due to interference by the surface return with the shallower mine echo.

## 6. CONCLUSION

The GPSAR system developed by Planning Systems Incorporated has been shown to be effective at detecting buried plastic anti-tank mines. The system performs well with the antennas elevated at twelve inches, but better at two inches. This is attributed to masking effect of the ground surface return and aggravated by surface moisture present during the test period. Further tests of the system will be scheduled at Army test sites in CY02 and the results will be published.